JOURNAL OF COMPUTATIONAL PHYSICS 74, 214–232 (1988)

A Posteriori Error Estimates in Finite Difference Techniques

D. W. KELLY, R. J. MILLS, AND J. A. REIZES

School of Mechanical and Industrial Engineering, University of New South Wales, Sydney, Australia 2033

AND

A. D. MILLER*

Centre for Mathematical Analysis, Australian National University, Canberra, Australia 2601

Received April 4, 1986; revised March 25, 1987

A technique is described which defines an upper bound for the effect of the truncation error on finite difference solutions to elliptic boundary value problems. This technique does not attempt to provide an estimate which can be used to correct the finite difference solution but rather to produce a guaranteed upper bound measure of the error which can be used to assess the quality of the solution. Application to two problems is given to demonstrate the basic features of the analysis which is implemented in a post-processing mode once the original solution has been completed. © 1988 Academic Press, Inc.

1. INTRODUCTION

The fundamental approach in most computational methods is to discretize the governing differential equations. The finite difference method is a classic example of this approach. Here a mesh is superimposed onto the computational domain and a solution sought at intersecting points on the mesh, commonly referred to as nodes. At these locations the governing equations are represented by discrete differential operators derived using Taylor series expansions. If the infinite Taylor series were retained, an exact solution would be realized for the problem. However, for practical reasons, the infinite series is usually truncated after the second-order term. This imposes an error which exists in all solutions which use the finite difference technique [1–3].

A procedure is described here which will provide an upper bound measure of the effect on the solution of all the trailing terms in the truncated Taylor series. This analysis was originally proposed for the finite element technique [4–6] but we show

* Present address: Division of Mathematics and Statistics, C.S.I.R.O., Adelaide, S.A. Australia 5064.

0021-9991/88 $3.00

it to be adaptable to finite difference procedures. Since this theory interprets the effect of residuals, it provides guidance for local solution refinement which will more fully capture the true physics of the problem.

Features of the analysis are highlighted in the following sections together with its application to two fundamental problems.

2. THEORY

Methods which employ the truncation error approach to error analysis either compare the solution from successive refinements of the mesh or evaluate directly the leading terms in the truncation error given by the Taylor series. These methods cannot be guaranteed to either overestimate or underestimate the contribution of the trailing terms in the Taylor series, but if convergence is monotonic, successive refinements will succeed in only progressing part of the way toward the exact solution [1]. However, a method developed for finite elements uses a complementary analysis to estimate the discretization error in the numerical solution [5]. This theory has been formulated using properties inherent in the finite element method to produce an estimate which yields a guaranteed upper bound on the discretization error. The complementary analysis is shown here to be adaptable to finite difference techniques producing a bounded measure of the truncation error in the solution.

The essential components in the error estimate are a measure of the distance from the numerical solution, $\bar{\phi}_h$, to the exact solution, ϕ, and the direction giving the change in nodal values when progressing from the numerical solution to the exact solution. In Fig. 1 we represent the discrete nodal values of the exact solution as the vector $\{\phi\}_{\text{exact}}$ and the nodal values of the numerical solution as the vector $\{\bar{\phi}_h\}$ in a two-dimensional space:

$$\text{The error,} \qquad \{\bar{e}\} = \{\phi\}_{\text{exact}} - \{\bar{\phi}_h\} \tag{1}$$

$$\text{is given by } \{\bar{e}\} = |c| \cdot \mathbf{d}, \tag{2}$$

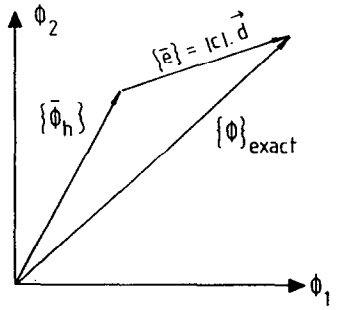

FIG. 1. Identification of the error in a numerical solution.

where **d** is a unit vector directed from the numerical solution toward the exact solution and $|c|$ is the magnitude or scaling factor defining the distance between the two solutions. The error estimate will require the estimation of both **d** and $|c|$.

To illustrate the application of the theory consider a simple elliptic problem in two dimensions, viz.,

$$\nabla^2\phi = -f \text{ on the domain } \Omega \tag{3}$$

with

$$\frac{\partial\phi}{\partial n} = g \text{ on the boundary } \partial\Omega.$$

Here $\phi = \phi(x, y)$ represents a continuous scalar potential function over the domain Ω, produced by a source term f over the domain and a Neumann condition g, imposed along the boundary $\partial\Omega$. The unit vector, **n**, has a direction defined normal to the boundary $\partial\Omega$ and is assumed positive outwards from the domain Ω.

Here a finite difference solution, $\bar{\phi}_h$, is sought to (3). The development of the theory which follows, however, requires that we propose a solution $\phi_h \in S_h$ which satisfies

$$B(\phi_h, \psi) = (f, \psi) + [g, \psi] \qquad \forall\psi \in S_h, \tag{4}$$

where ψ for the moment is arbitrary and S_h is the space of admissible functions. Here

$$B(u, v) = \iint_\Omega \left[\frac{\partial u}{\partial x}\frac{\partial v}{\partial x} + \frac{\partial u}{\partial y}\frac{\partial v}{\partial y}\right] d\Omega \tag{5}$$

$$(f, v) = \int_\Omega f \cdot v \, d\Omega \tag{6}$$

$$[g, v] = \oint_{\partial\Omega} g \cdot v \, ds, \tag{7}$$

where ds is an element of the boundary curve $\partial\Omega$.

The difference between the exact solution, ϕ, and the solution, ϕ_h, is defined as

$$e = \phi - \phi_h. \tag{8}$$

The energy norm of the error defined by (8) is given by

$$B(e, e) = B(\phi - \phi_h, \phi - \phi_h). \tag{9}$$

Expanding the right-hand side of (9) yields

$$B(e, e) = B(\phi, \phi) - 2B(\phi, \phi_h) + B(\phi_h, \phi_h). \tag{10}$$

Here $B(\phi, \phi)$ is the energy norm of the exact solution and $B(\phi_h, \phi_h)$ the energy norm of the discrete solution. The cross product, $B(\phi, \phi_h)$, is simplified using integration by parts to produce

$$B(\phi, \phi_h) = \oint_{\partial\Omega} \phi_h \frac{\partial \phi}{\partial n}\, ds - \iint_{\Omega} \phi_h \left(\frac{\partial^2 \phi}{\partial x^2} + \frac{\partial^2 \phi}{\partial y^2} \right) dx\, dy. \tag{11}$$

If the governing differential equations, defined by (3), are imposed onto (11) for the Neumann problem then

$$B(\phi, \phi_h) = [g, \phi_h] + (f, \phi_h). \tag{12}$$

By definition, the solution ϕ_h satisfies Green's identity,

$$B(\phi_h, \phi_h) = [g, \phi_h] + (f, \phi_h). \tag{13}$$

It then follows from (12) and (13) that

$$B(\phi, \phi_h) = B(\phi_h, \phi_h). \tag{14}$$

Substituting the identity from (14) into (10) gives

$$B(\phi, \phi) = B(\phi_h, \phi_h) + B(e, e). \tag{15}$$

We note that $B(e, e)$ provides a measure in the energy of the difference between the solution ϕ_h and the exact solution ϕ. We also note that since ϕ_h satisfies (14)

$$B(e, \phi_h) = B(\phi - \phi_h, \phi_h) = B(\phi, \phi_h) - B(\phi_h, \phi_h) = 0,$$

that is, the error in the proposed solution ϕ_h is orthogonal in the energy norm to ϕ_h.

In practical applications the error in the solution is not known *a priori* and so the error norm $B(e, e)$ cannot be evaluated directly from the numerical solution ϕ_h. To overcome this problem Kelly [5] has proposed to overestimate the truncation error in ϕ_h so as to provide an upper bound on the exact solution ϕ.

This can be performed if a complementary variational theory is employed which will produce an upper bound estimate $B_u(e, e)$ of $B(e, e)$. Clearly then from (15) we obtain an upper bound for $B(\phi, \phi)$

$$B(\phi, \phi) \leqslant B(\phi_h, \phi_h) + B_u(e, e). \tag{16}$$

The following section describes the method used to evaluate the two terms on the right-hand side of (16).

2.1. *Energy Norm of the Solution*

In the above discussion, the validity of (15) and therefore (16) is predicated on the requirement that ϕ_h will satisfy Green's identity, (13). For example, this

property is explicit in finite element procedures and any solution using this method will satisfy Green's identity *a priori* [7].

Our research is directed toward adapting the complementary analysis to the finite difference technique. This numerical method is not based on integral relations such as (4) but is derived from a Taylor series expansion about local nodes. Hence if (16) is implemented for a finite difference solution, $\bar{\phi}_h$, a bounded estimate of the energy in the exact solution cannot be guaranteed. Therefore, for a finite difference solution of (3), (16) is rewritten as

$$B(\phi, \phi) \leqslant B(\bar{\phi}_h, \bar{\phi}_h) + [B(\phi_h, \phi_h) - B(\bar{\phi}_h, \bar{\phi}_h)] + B_u(e, e) \tag{17}$$

in which $[B(\phi_h, \phi_h) - B(\bar{\phi}_h, \bar{\phi}_h)]$ is some measure of the discrepancy between the finite difference solution, $\bar{\phi}_h$ and ϕ_h. We note here that the measure proposed in (17), and implemented in the analysis which follows, is applicable to any solution and is not restricted to a finite difference analysis.

The evaluation of the first two terms on the right-hand side of (17) is described in the following. The first term is the energy norm of the finite difference solution, $\bar{\phi}_h$. This is defined by (5) as

$$B(\bar{\phi}_h, \bar{\phi}_h) = \iint_\Omega \left(\frac{\partial \bar{\phi}_h}{\partial x} \frac{\partial \bar{\phi}_h}{\partial x} + \frac{\partial \bar{\phi}_h}{\partial y} \frac{\partial \bar{\phi}_h}{\partial y} \right) dx\, dy. \tag{18}$$

In the finite difference technique, $\bar{\phi}_h$, and its derivatives are thought of as discrete values at nodal points on the mesh and not as continuous functions implied by (18). To evaluate the energy norm we introduce into the analysis a linear interpolant of $\bar{\phi}_h$. Then $\bar{\phi}_h$ exists in S_h, permitting the explicit evaluation of $B(\bar{\phi}_h, \bar{\phi}_h)$ and the substitution of $\bar{\phi}_h$ for ψ in (4). The linear interpolant is the simplest interpolation of the solution between the nodal values. It is chosen here to ensure that the complementary problem in Section 2.2 is solved with no greater accuracy than the finite difference solution to the original problem so that a conservative bounding envelope indicating the error in the exact solution should be achieved.

Next consider the quantity within square brackets in (17). This term can be evaluated using the following

$$B(\phi_h - \bar{\phi}_h, \phi_h - \bar{\phi}_h) = B(\phi_h, \phi_h) - 2B(\phi_h, \bar{\phi}_h) + B(\bar{\phi}_h, \bar{\phi}_h). \tag{19}$$

Rearranging (19) gives

$$\begin{aligned} B(\phi_h, \phi_h) - B(\bar{\phi}_h, \bar{\phi}_h) = {} & 2[B(\phi_h, \bar{\phi}_h) - B(\bar{\phi}_h, \bar{\phi}_h)] \\ & + B(\phi_h - \bar{\phi}_h, \phi_h - \bar{\phi}_h) \end{aligned} \tag{20}$$

which is the measure sought in (17). Here $B(\bar{\phi}_h, \bar{\phi}_h)$ can be directly evaluated since $\bar{\phi}_h$ is the finite difference solution. However, $B(\phi_h, \bar{\phi}_h)$ cannot be evaluated directly since ϕ_h has not been defined. This problem is resolved since ϕ_h satisfies the property given by (4) in which ψ is replaced with the finite difference solution, $\bar{\phi}_h$.

Therefore

$$B(\phi_h, \bar{\phi}_h) = (f, \bar{\phi}_h) + [\bar{\phi}_h, g]$$
$$= \int_\Omega f \cdot \bar{\phi}_h \, d\Omega + \oint_{\partial\Omega} \bar{\phi}_h \cdot g \, ds \tag{21}$$

and is therefore evaluated as an integral of known data on the boundary.

The measure given in (20) will be implemented directly in (17) because the last term on the right-hand side of this expression will be cancelled by a similar term arising in the evaluation of $B_u(e, e)$ in the next section. At this intermediate stage, however, we note that $[B(\phi_h, \phi_h) - B(\bar{\phi}_h, \bar{\phi}_h))]$ provides a measure of the lack of satisfaction of Green's identity by the finite difference solution because ϕ_h is a solution satisfying Green's identity and $\bar{\phi}_h$ the finite difference solution. It will now be shown that the last term on the right-hand side of (20) is negligible so that (20) can be used directly as an indicator of the effect of imposing Green's identity (for example, implementing a 9-point finite element differencing grid rather than the 5-point finite difference grid).

Here the energy norm of $(\phi_h - \bar{\phi}_h)$ is

$$B(\phi_h - \bar{\phi}_h, \phi_h - \bar{\phi}_h) = \|\phi_h - \bar{\phi}_h\|_E^2 = \varepsilon \qquad \text{(say)}. \tag{22}$$

In addition, the first term on the right-hand side of (20) can be rearranged as

$$B(\phi_h, \bar{\phi}_h) - B(\bar{\phi}_h, \bar{\phi}_h) = B(\phi_h - \bar{\phi}_h, \bar{\phi}_h)$$
$$\approx \|\phi_h - \bar{\phi}_h\|_E \cdot \|\bar{\phi}_h\|_E$$
$$= \Delta \qquad \text{(say)} \tag{23}$$

if cancellation in the integral is negligible. Then

$$\frac{\varepsilon}{\Delta} \approx \frac{\|\phi_h - \bar{\phi}_h\|_E}{\|\bar{\phi}_h\|_E}. \tag{24}$$

It follows, for a particular discrete solution of (3), as might be given by finite difference techniques for example, that in the limit

$$\lim_{h \to 0} \frac{\varepsilon}{\Delta} \to 0$$

in which h is the mesh size. Thus (20) becomes

$$B(\phi_h, \phi_h) - B(\bar{\phi}_h, \bar{\phi}_h) = \left[2 + O\left(\frac{\varepsilon}{\Delta}\right)\right] \cdot [B(\phi_h, \bar{\phi}_h) - B(\bar{\phi}_h, \bar{\phi}_h)] \tag{25}$$

and the right-hand side of (20) can be explicitly evaluated to give a measure of the error in the finite difference solution if Green's identity is not satisfied.

Note that (17) can be written as

$$B(\phi, \phi) \leqslant B(\bar{\phi}_h, \bar{\phi}_h) + 2[B(\phi_h, \bar{\phi}_h) - B(\bar{\phi}_h, \bar{\phi}_h)] + [B_u(e, e) + B(\phi_h - \bar{\phi}_h, \phi_h - \bar{\phi}_h)]. \tag{26}$$

Equation (26) will be used in Section 2.3 to define the distance $|c|$ in (2). However, an expression for $B_u(e, e)$ must first be derived.

2.2. *The Complementary Error Eestimate for* $B(e, e)$

Earlier the quantity, $B(e, e)$, was introduced to represent the norm of the discretization error in ϕ_h. To perform a complementary analysis, this error is identified as the response to a residual forcing system which has two contributions. The first is a domain residual, r, representing the lack of satisfaction of the governing differential equations on the domain Ω_i. For example, the exact solution ϕ in Fig. 2 satisfies

$$\frac{\partial^2 \phi}{\partial x^2} + \frac{\partial^2 \phi}{\partial y^2} + f = 0.$$

For the discrete solution, ϕ_h,

$$\frac{\partial^2 \phi_h}{\partial x^2} + \frac{\partial^2 \phi_h}{\partial y^2} + f = r \neq 0,$$

where a linear interpolant in ϕ_h between nodes is assumed.

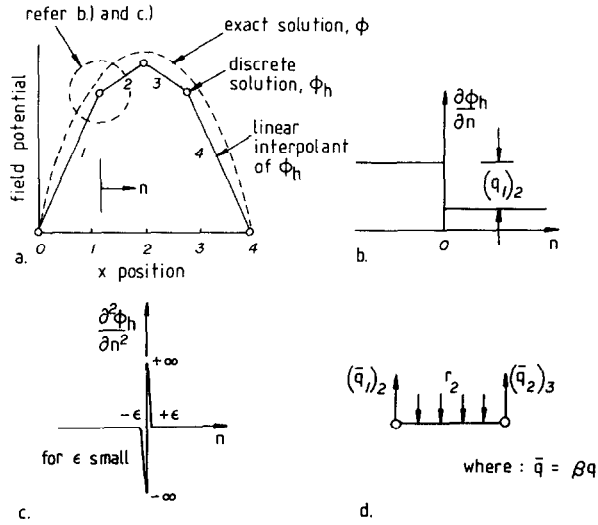

FIG. 2. The residual force system on an isolated element: (a) definition of terms; (b) jump in the slope of the linear interpolant of ϕ_h across boundary; (c) discontinuity in the 2nd derivative of the linear interpolant of ϕ_h across the element boundary; (d) residual forcing system on element 2.

The second contribution is an interface residual q produced by the jump in slope of ϕ_h between adjacent elements, ϕ_h being the linear interpolant between the nodal values as described earlier. Here an element is defined as a region enclosed by four neighboring nodes on a square mesh designated as Ω_i. Again for the linear element at the boundary,

$$\frac{\partial^2 \phi_h}{\partial x^2} + \frac{\partial^2 \phi_h}{\partial y^2} + f = r^*,$$

where r^* is a singular residual defined such that

$$\int_{-\varepsilon}^{+\varepsilon} r^* \, dn = \Delta \frac{\partial \phi}{\partial n} = q$$

with n normal to the element edge and its origin located at the interface (Figs. 2a, b, c).

The response to these residual forces is the error in the numerical solution. To ensure that $B(e, e)$ is overestimated it is possible to implement the complementary analysis defined in [8]. If the residuals are divided into self-equilibrating systems on each element the analysis can proceed element by element since the flows do not interact with those of their neighboring counterparts. The condition for self-equilibration becomes

$$\oint_{\partial\Omega_i} \bar{q} \, ds - \int_{\Omega_i} r \, d\Omega = 0 \tag{27}$$

in which $\bar{q}$ represents a fraction of the total interface residual which has been partitioned between the current and adjacent element boundaries in order to assure self-equilibration (Fig. 2d). This partitioning results in the definition of splitting factors, β, on each interface such that βq is allocated to one element and $(1-\beta)q$ to its neighbor across the interface. To determine the factors β for the examples given in this paper, a conjugate gradient search algorithm [9] was implemented which adjusts the splitting factors on the adjacent element boundaries in order to minimize the sum of squares of the residual in (27), viz.,

$$R = \sum \left[\oint_{\partial\Omega_i} \bar{q} \, ds - \int_{\Omega_i} r \, d\Omega \right]^2. \tag{28}$$

Experiments with this technique on several sample problems, indicate that R can be driven to zero to within machine accuracy.

For a linear interpolant of ϕ_h over an element, the interface residual produced is a linear function in x and y along the edges of the element. To proceed with the complementary analysis a continuous function of Q over each element such that

$Q_x = \partial e/\partial x$ and $Q_y = \partial e/\partial y$ is defined. In order to guarantee a bounded estimate of the error, Q must satisfy the following constraints [7],

$$\nabla \cdot Q = r \qquad \text{on the domain } \Omega_i \tag{29}$$

and

$$Q \cdot \mathbf{n} = \bar{q} \qquad \text{on the boundary } \partial\Omega_i.$$

For the purpose of the examples presented in this paper, a function similar to that in [5] was used, viz.,

$$\begin{aligned} Q_x &= \alpha_1 x^2 - 2\alpha_2 xy + \left(\alpha_3 + \frac{r}{2}\right) x + \alpha_4 + \alpha_5 y \\ Q_y &= -2\alpha_1 xy + \alpha_2 y^2 - \left(\alpha_3 - \frac{r}{2}\right) y + \alpha_6 + \alpha_7 x \end{aligned} \tag{30}$$

which satisfies (29) *a priori* if r is a constant.

The constants α_1, α_2, α_3, α_4, α_5, α_6, α_7 in (30) are evaluated using values of the interface residual at selected points around the element bounary (Fig. 3). Once the constants in (30) have been determined on the current element, the local norm of the error is calculated using

$$\|e\|^2_{\Omega_i} = \iint_{\Omega_i} [(Q_x)^2 + (Q_y)^2]\, dx\, dy. \tag{31}$$

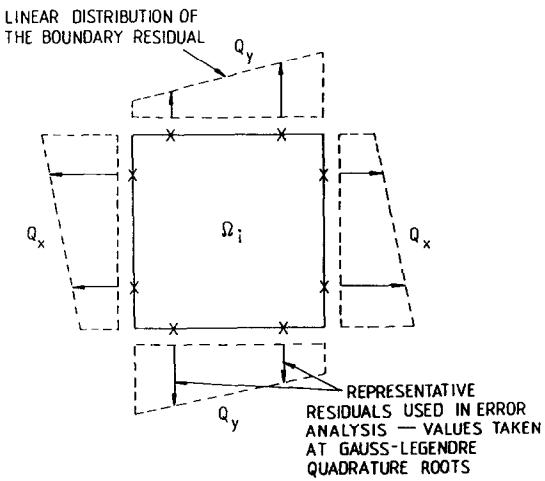

FIG. 3. Assumed distribution of the interface residual.

The energy of the error for the solution is obtained by suming the local estimate, made using (31), over the domain Ω, i.e.,

$$B_u(e, e) = \sum_{i=1}^{n} \|e\|^2_{\Omega_i} \tag{32}$$

in which N is the number of "elements" on the solution domain Ω.

It can be shown (for example, [5] or [8]) that (31) and (32) produce a guaranteed upper bound on the error norm for the solution provided the residual system on each "element" self-equilibrates and r is constant.

In this analysis $e = \phi - \phi_h$. To implement this theory on a finite difference solution $\bar{\phi}_h$ define

$$\bar{e} = \phi - \bar{\phi}_h.$$

After substituting for $B(\phi_h, \phi_h)$ from (20), (15) becomes

$$\begin{aligned} B(\phi, \phi) = B(\bar{\phi}_h, \bar{\phi}_h) + 2[B(\phi_h, \bar{\phi}_h) - B(\bar{\phi}_h, \bar{\phi}_h)] \\ + B(\phi_h - \bar{\phi}_h, \phi_h - \bar{\phi}_h) + B(e, e). \end{aligned}$$

The error norm for the finite difference solution $B(\bar{e}, \bar{e})$ is introduced onto the right-hand side of the above equation as

$$\begin{aligned} B(\phi, \phi) = B(\bar{\phi}_h, \bar{\phi}_h) + 2[B(\phi_h, \bar{\phi}_h) - B(\bar{\phi}_h, \bar{\phi}_h)] \\ + B(\phi_h - \bar{\phi}_h, \phi_h - \bar{\phi}_h) + B(\bar{e}, \bar{e}) + [B(e, e) - B(\bar{e}, \bar{e})]. \end{aligned} \tag{33}$$

Expanding the last term in square brackets

$$\begin{aligned} B(e, e) - B(\bar{e}, \bar{e}) &= B(\phi - \phi_h, \phi - \phi_h) - B(\phi - \bar{\phi}_h, \phi - \bar{\phi}_h) \\ &= B(\phi, \phi) - 2B(\phi, \phi_h) + B(\phi_h, \phi_h) \\ &\quad - B(\phi, \phi) + 2B(\phi, \bar{\phi}_h) - B(\bar{\phi}_h, \bar{\phi}_h). \end{aligned}$$

From (14) $B(\phi, \phi_h) = B(\phi_h, \phi_h)$, therefore

$$B(e, e) - B(\bar{e}, \bar{e}) = -B(\phi_h, \phi_h) + 2B(\phi, \bar{\phi}_h) - B(\bar{\phi}_h, \bar{\phi}_h).$$

Finally since $\bar{\phi}_h \in S_h$ and can be used as the function ψ in (4)

$$B(\phi, \bar{\phi}_h) = B(\phi_h, \bar{\phi}_h),$$

with the result

$$\begin{aligned} B(e, e) - B(\bar{e}, \bar{e}) &= -B(\phi_h, \phi_h) + 2B(\phi_h, \bar{\phi}_h) - B(\bar{\phi}_h, \bar{\phi}_h) \\ &= -B(\phi_h - \bar{\phi}_h, \phi_h - \bar{\phi}_h). \end{aligned}$$

Thus (33) becomes

$$B(\phi, \phi) - B(\bar{\phi}_h, \bar{\phi}_h) = 2[B(\phi_h, \bar{\phi}_h) - B(\bar{\phi}_h, \bar{\phi}_h)] + B(\bar{e}, \bar{e}). \tag{34}$$

By using the complementary theory to produce an upper bound estimate of $B(\bar{e}, \bar{e})$, (34) becomes

$$B(\phi, \phi) - B(\bar{\phi}_h, \bar{\phi}_h) \leqslant 2[B(\phi_h, \bar{\phi}_h) - B(\bar{\phi}_h, \bar{\phi}_h)] + B_u(\bar{e}, \bar{e}), \tag{35}$$

where $B_u(\bar{e}, \bar{e})$ is obtained by substituting $\bar{e}$ for e in (32). The terms on the right-hand side of (35) are evaluated from the finite difference solution using Eq. (18), (21), (31), and (32) and will be used in the next section to produce an upper bound estimate of $|c|$ defined in (2).

2.3. *Local Error Estimation*

In the previous section a measure of the discretization error was introduced in terms of the norm $B(\cdot, \cdot)$. In addition, the distribution of this error over the solution domain was identified by analyzing the mesh as a series of self-contained elements whose residual forcing system is required to self-equilibrate. Clearly it is necessary to define a measure of the pointwise error in $\bar{\phi}_h$ and its derivatives.

Here it is proposed to implement a scaling procedure to estimate the error pointwise. To achieve this the direction of the error, **d** in (2), must be identified. Obviously this direction can be obtained by a re-solution of the differential equations on a more refined or more coarse mesh. Solution on the more coarse mesh is clearly more desirable since it is less time consuming. The direction thus obtained can be expected to be acurate **only** when the grid is sufficiently fine for the solution to have entered the asymptotic range. This method has been adopted into this analysis. No additional expense in using this technique is incurred if the finite difference algorithm has already derived a solution on a coarse mesh to accelerate its convergence.

If $\bar{\phi}_{2h}$ is the finite difference solution on a coarse mesh, the refined solution $\bar{\phi}_h$, can be scaled to $\hat{\phi}$ using

$$\hat{\phi} = \bar{\phi}_h + c(\bar{\phi}_h - \bar{\phi}_{2h}) \tag{36}$$

in which c is the scaling factor (or distance measure) to be evaluated. The energy norm of $\hat{\phi}$ is defined

$$(f, \hat{\phi}) + [g, \hat{\phi}] = B(\bar{\phi}_h, \bar{\phi}_h) + 2[B(\phi, \bar{\phi}_h) - B(\bar{\phi}_h, \bar{\phi}_h)] + B_u(\bar{e}, \bar{e}), \tag{37}$$

where $(f, \hat{\phi})$ and $[g, \hat{\phi}]$ are evaluated using (6) and (7). If $\hat{\phi}$ in (36) is substituted into (37), and (21) is implemented, an expression for the scaling factor is given by

$$c = \left(\frac{B_u(\bar{e}, \bar{e}) + [B(\phi_h, \bar{\phi}_h) - B(\bar{\phi}_h, \bar{\phi}_h)]}{B(\phi_h, \bar{\phi}_h) - B(\phi_{2h}, \bar{\phi}_{2h})} \right) \tag{38}$$

with the terms in the denominator evaluated using (21). The solution $\hat{\phi}$ will then have an energy norm equal to the upper bound on the right-hand side of (37).

3. EXAMPLES

Here two examples are presented to demonstrate the ability of the error analysis to produce a bounded estimate of the error in the finite difference solution. In addition, two difference operators are introduced to substantiate the procedure used to sense the satisfaction of Green's identity in the solution. Data from a finite element analysis of these examples has been used to verify the findings in (25).

The two examples presented differ in the distribution of discretization error over their respective domains and hence produce separate challenges for the theory. Here the first example exhibits a relatively uniform distribution of error over the solution domain whereas the second example is characterized by highly localized regions of discretization error.

3.1. *Membrane Analogy on a Square Domain*

The problem analyzed in this example is defined in Fig. 4. Here a solution is sought to the Poisson equation for the dependent variable ϕ over the domain Ω. A constant source term, f, is imposed over the domain, Ω and homogeneous Dirichlet conditions enforced on the boundary, $\partial\Omega$. For this analysis a value of $f = 1$ has been selected for the source term.

A finite difference solution to the governing differential equations was obtained by implementing a 5-node operator (Fig. 5a) over the domain, Ω. The resultant set of linear difference equations was solved by accelerated Gauss–Siedel (SOR) iteration using overrelaxation. Convergence of the solution occurred when the maximum change in $\bar{\phi}_h$ over the domain fell within $|1.0 \times 10^{-5}|$. The optimum relaxation factor for the chosen mesh size was obtained from [10]. Three mesh sizes were examined for this example. They included a coarse (5×5), medium (9×9) and fine (17×17) grid.

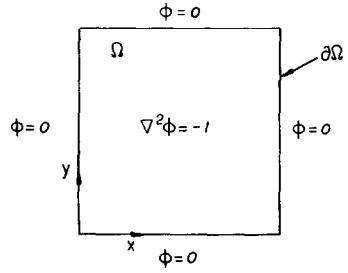

FIG. 4. Definition of the membrane analogy problem.

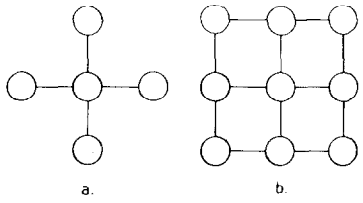

FIG. 5. Structure of the 2nd-order finite difference operators.

Table I presents the results of this analysis. The first column gives the energy norm of the finite difference solution evaluated using (18). The second column gives the norm $B(\phi_h, \bar{\phi}_h)$ evaluated from the finite difference solution using (21). The third column contains the norm $B_u(\bar{e}, \bar{e})$ evaluated using the procedures described in Section 2.2. A measure of the efficiency of (35) in providing an upper bound estimate of the required distance measure $|c|$ between the finite difference solution $\bar{\phi}_h$ and the exact solution ϕ is given by Θ in the fourth column. The effectivity index, Θ, is defined from (35) as

$$\Theta = \left[\frac{2[B(\phi_h, \bar{\phi}_h) - B(\bar{\phi}_h, \bar{\phi}_h)] + B_u(\bar{e}, \bar{e})}{B(\phi, \phi) - B(\bar{\phi}_h, \bar{\phi}_h)}\right]. \tag{39}$$

Clearly a value of Θ greater than one but also close to one is needed. The energy norm for the "exact' solution $B(\phi, \phi)$ required in (39) was evaluated using Richardson's extrapolation on the numerical results in the fifth column of Table I.

To illustrate the above procedures consider the results for the finite difference solution on the (5×5) mesh in Table I. Here the upper bound estimate for the distance $|c|$ in (2) is given by

$$2(288.08 - 259.60) + 58.39 = 115.35.$$

TABLE I

Error Analysis for the Membrane Analogy Problem

Grid	$B(\bar{\phi}_h, \bar{\phi}_h)$	$B(\phi_h, \bar{\phi}_h)$	$B_u(\bar{e}, \bar{e})$	Θ	$B(\phi_h, \phi_h)$	$2 + O\left(\frac{\varepsilon}{\Delta}\right)$	Bound from (35)
Coarse 5×5	259.60	288.08	58.39	1.2560	319.74	2.11	115.35
Medium 9×9	325.40	334.24	10.21	1.0710	343.34	2.03	27.89
Fine 17×17	344.68	347.02	2.17	1.0133	349.40	2.02	6.85
"Exact"					351.44		

These values are entered in the last column of Table I. The exact distance of $|c|$ from our knowledge of the "exact" solution to this problem is

$$351.44 - 259.60 = 91.84,$$

giving the effectivity index

$$\Theta = \frac{115.35}{91.84} = 1.2560.$$

To independently test the factor $[2 + O(\varepsilon/\Delta)]$ in (25), the fifth column in Table I gives a solution satisfying (4). This result was obtained using a 9-point scheme giving directly the Galerkin finite element solution ϕ_h. For the coarse (5×5) mesh the factor applied to the measure $[B(\phi_h, \phi_h) - B(\phi_h, \phi_h)]$ in (25) is

$$\left[2 + O\left(\frac{\varepsilon}{\Delta}\right)\right] = \frac{319.74 - 259.60}{288.08 - 259.60} = 2.11.$$

The error estimate $\|\bar{e}\|^2_{\Omega_i}$ is evaluated independently on each subregion bounded by four nodes using (31) and summed to give the total norm, $B_u(\bar{e}, \bar{e})$. In finite element work the distribution of this error norm on each element has been used to guide local adaptive refinement of the mesh (e.g., [4]). The contour plots in Fig. 6 indicate that the truncation error for this problem is relatively uniformly distributed compared, for example, to the same plot given for the next example.

After implementing the complementary analysis, the finite difference solution was scaled to the predicted energy bound using the procedures outlined in the previous section (Fig. 7a, b). Here the scaled solution converged monotonically toward the exact solution as the mesh was uniformly refined over the domain. The finite difference analysis on the fine (17×17) mesh produced numerical results which were close to the exact solution over the domain Ω. Thus, pointwise refinements to the solution produced a negligible change between the original numerical results and the exact solution (Fig. 7b).

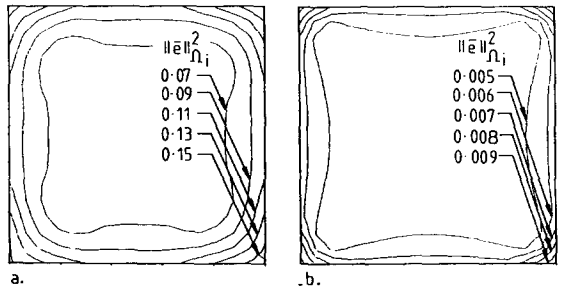

FIG. 6. Contours of local error norm for the membrane problem: (a) medium (9×9) mesh; (b) fine (17×17) mesh.

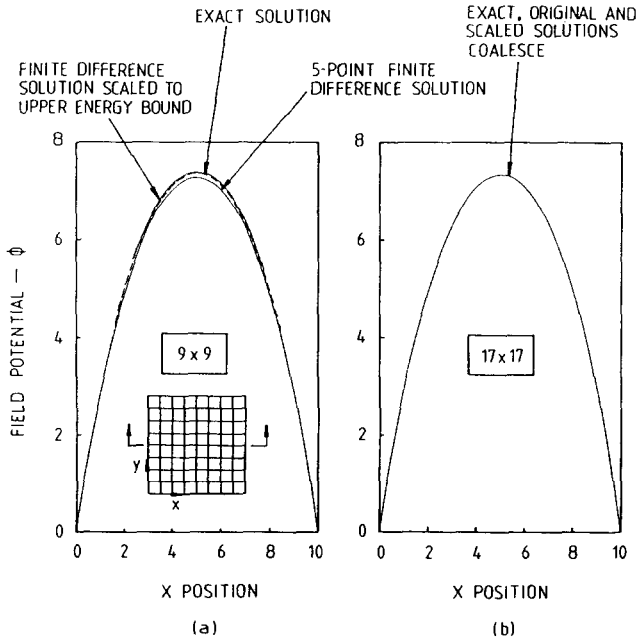

FIG. 7. Pointwise refinements to the membrane analogy problem.

3.2. *Two-Dimensional Inviscid Flow about a Bluff Body*

In the first example a problem was examined which had a relatively uniform distribution of the discretization error over the solution domain. Here a more general form of problem is considered which has highly localized regions of truncation error. This example is defined in Fig. 8a. In this problem the Laplace equation is solved to find the distribution of velocity potential, ϕ, around a bluff body contained between two impermeable surfaces. The flow into and out of the control volume, Ω, is constrained to the horizontal plane. Neumann boundary conditions are enforced on all surfaces of the domain including the boundaries adjacent to the bluff body in order to satisfy the no-flow condition at the boundary interface. A cartesian mesh system was used to conform to the geometry of the solution domain (Fig. 8b).

Two second-order finite difference operators were used to verify the theory. The first is the classical 5-node scheme (Fig. 5a) used by most researchers in finite difference methods [1, 10, 11]. The second approach implements a 9-node operator (Fig. 5b) which has properties found in the local stiffness matrices of the finite element method [12]. However, the use of the 9-node operator in this research does not mimic the finite element analysis since the boundary conditions for this problem are enforced in a manner consistent with conventional finite difference procedures [10, 11]. Using this approach, two different finite difference solutions

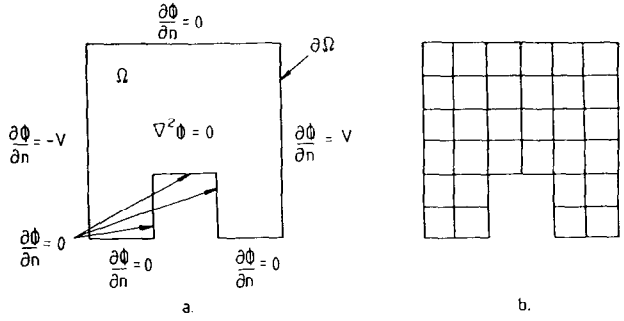

FIG. 8. Problem definition and mesh structure.

may be generated for the same problem. This tests whether the findings in (25) are general enough to apply to an arbitrary difference operator or if the analysis is confined to a particular class of difference scheme.

The distribution of velocity potential, ϕ, for this example was examined on a coarse (7×7), medium (13×13), and fine (25×25) mesh by implementing a direct solver on the banded system of linear equations generated by applying the difference operators at each node in the solution domain, Ω. The numerical solutions to the governing equations were analyzed using the theory proposed earlier.

The results in Table II again indicate that an accurate estimate of the distance $|c|$ in (2) can be obtained by the procedures recommended in this paper. The column for Θ indicates a close upper bound on $|c|$ has been achieved and the second last column, which contains the factor $[2 + O(\varepsilon/\Delta)]$, verifies the findings in (25). The factor Θ remains approximately constant because the error prediction and the actual error are converging to zero at the same rate.

TABLE II

Error Analysis of the Flow Field around a Bluff Body Evaluated Using a 5-Point 2nd-Order Finite Difference Operator

Grid	$B(\tilde{\phi}_h, \tilde{\phi}_h)$	$B(\phi_h, \tilde{\phi}_h)$	$B_u(\bar{e}, \bar{e})$	Θ	$B(\phi_h, \phi_h)$	$2 + O\left(\frac{\varepsilon}{\Delta}\right)$	Bound from (35)
Coarse 7×7	114310	119259	4523	1.0542	125253	2.21	14421
Medium 13×13	122243	124457	1761	1.0769	126933	2.12	6189
Fine 25×25	125650	126576	680	1.0821	127582	2.09	2532
"Exact"					127990		

TABLE III
Error Analysis of the Flow Field around
a Bluff Body Evaluated Using
a 9-Point 2nd-Order Finite Difference Operator

Grid	$B(\bar{\phi}_h, \bar{\phi}_h)$	$B(\phi_h, \bar{\phi}_h)$	$B_u(\bar{e}, \bar{e})$	Θ	$B(\phi_h, \phi_h)$	$2+O\left(\frac{\varepsilon}{\Delta}\right)$	Bound from (35)
Coarse 7×7	121054	123081	4481	1.2305	125253	2.07	8535
Medium 13×13	125187	126046	1659	1.2048	126933	2.03	3377
Fine 25×25	126876	127226	621	1.1858	127582	2.02	1321
"Exact"					127990		

A clearer picture of the monotonic convergence of the solution is given by the results in last column in Table II. This quantity is evaluated from the right-hand side of (35) and provides a measure of the accuracy between any two solutions. For example, comparison between the results in Tables II and III for a particular mesh show conclusively that the 9-point operator has produced more accurate results than those obtained using the conventional 5-point scheme.

In an approach similar to that of the previous example, a Galerkin finite element method was used to produce a reference solution, and hence energy norm, which satisfies Green's identity. This norm is used as a measure against which the results from the finite difference analysis are compared in order to verify our findings in (25). The energy norm for the exact solution was estimated using Richardson's extrapolation of the finite element results for the three different mesh sizes given in Tables II and III.

The complementary analysis was implemented for the finite difference method using both operators. This produced distributions of the discretization error over the solution domain (Fig. 9). As expected, high localized error norms were obtained

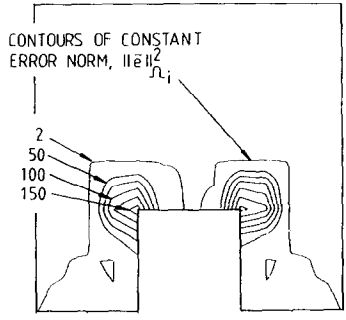

FIG. 9. Contours of local error norm for the 5-point finite difference solution to the bluff body example.

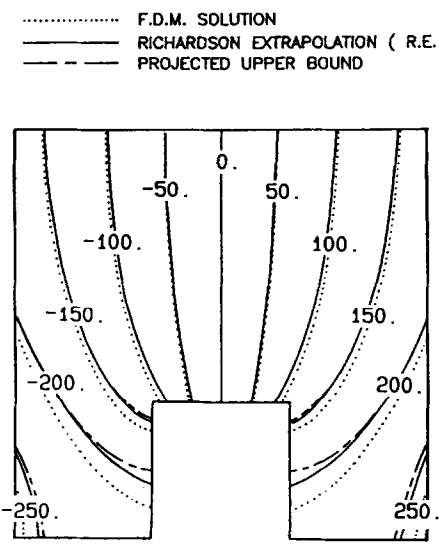

FIG. 10. Pointwise refinements to the bluff body example.

at the corners of the bluff body. This result reinforces confidence in the complementary analysis to reflect the correct distribution of error in a numerical solution.

The original finite difference solution, $\bar{\phi}_h$, on the medium (13×13) mesh was extrapolated to the bounds given by the complementary analysis using the scaling procedure described earlier. Results from the coarse mesh (7×7) solution were used in conjuction with the medium mesh data in order to evaluate the scaling factor defined by (38). The bounded results are presented in Fig. 10, where Richardson's extrapolation was used on the original numerical solutions and the result presented for reference purposes.

4. CONCLUSIONS

A method has been proposed which estimates the magnitude of all the terms in the truncated Taylor series and the influence of this error on the finite difference solution. The analysis guarantees a bounded estimate in the energy norm, of the truncation error provided the theory is implemented exactly. Preliminary research indicates that the numerically implemented bounds are in close proximity to the exact solution for reasonably coarse grids and show excellent comparison with further refinements to the mesh.

In addition, (25) provides a measure of the distance from a finite difference solution to one that satisfies Green's identity. This latter class of solution includes the finite element technique, among others. The measure is evaluated from the finite difference results and does not require any re-solution. Preliminary results suggest

that this method is independent of the type of difference operator used to solve the governing differential equations. We note here that this research has chosen to apply (25) to solutions generated by the finite difference technique. However, it should be realized that this equation has a more general application to any numerical solution. The authors are investigating the use of the local errors to guide the placement of the grid points using transformations based on body-fitted coordinates. The error contours in Fig. 9 will be used to define the local mesh density. The use of the energy of the error to define the mesh layout has been verified in the finite element method [4] and the benefits should transfer to the finite difference technique.

Implementation of the analysis proposed here on two fundamental problems has produced encouraging results from this initial research.

REFERENCES

1. P. J. ROACHE, *Computational Fluid Dynamics* (Hermosa, Albuquerque, NM, 1976).
2. R. S. HIRSH, *J. Comput. Phys.* **19**, 90 (1975).
3. K. Y. FUNG, J. TRIPP, AND B. GOBLE, "Adaptive Refinement with Truncation Error Injection," Presentation given at the School of Mechanical Engineering, University of Sydney, Australia, December 12, 1984 (unpublished).
4. I. BABUSKA AND W. C. RHEINBOLDT, *Int. J. Numer. Methods* **12**, 1597 (1978).
5. D. W. KELLY, *Int. J. Numer. Methods* **20**, 1491 (1984).
6. D. W. KELLY, "Self-Equilibration of Residuals and Upper Bound Error Estimates for Finite Element Methods," in *Accuracy Estimates and Adaptive Refinements in Finite Element Computations*, edited by I. Babuska, E. R. Oliveria, and O. C. Zienkiewicz (Wiley, New York, 1986).
7. J. T. ODEN AND J. N. REDDY, *Variational Methods in Theoretical Mechanics* (Springer-Verlag, Berlin, 1976).
8. R. D. MILNE, *Applied Functional Analysis: An Introductory Treatment* (Pitman, Boston, 1980).
9. J. L. KUESTER AND J. H. MIZE, *Optimization Techniques in Fortran* (McGraw-Hill, New York, 1973).
10. B. CARNAHAN, H. A. LUTHER, AND J. O. WILKES, *Applied Numerical Methods* (Wiley, New York, 1969).
11. G. E. FORSYTHE AND W. R. WASOW, *Finite Difference Methods for Partial Differential Equations* (Wiley, New York, 1960).
12. J. J. CONNOR AND C. A. BREBBIA, *Finite Element Techniques for Fluid Flow* (Newnes–Butterworths, London, 1978).